

Quantized large-bias current in the anomalous Floquet-Anderson insulator

Arijit Kundu^{1,2}, Mark Rudner,³ Erez Berg,^{4,5} and Netanel H. Lindner²¹Department of Physics, Indian Institute of Technology Kanpur, Kanpur 208016, India²Physics Department, Technion, 320003 Haifa, Israel³Niels Bohr International Academy and Center for Quantum Devices, University of Copenhagen, 2100 Copenhagen, Denmark⁴Department of Condensed Matter Physics, Weizmann Institute of Science, Rehovot 76100, Israel⁵Department of Physics, University of Chicago, Chicago, Illinois 60637, USA

(Received 24 September 2017; revised manuscript received 3 June 2018; published 8 January 2020)

We study two-terminal transport through two-dimensional periodically driven systems in which all bulk Floquet eigenstates are localized by disorder. We focus on the anomalous Floquet-Anderson insulator (AFAI) phase, a topologically nontrivial phase within this class, which hosts topologically protected chiral edge modes coexisting with its fully localized bulk. We show that the unique properties of the AFAI yield remarkable far-from-equilibrium transport signatures: for a large bias between leads, a quantized amount of charge is transported through the system each driving period. Upon increasing the bias, the chiral Floquet edge mode connecting source to drain becomes fully occupied and the current rapidly approaches its quantized value.

DOI: 10.1103/PhysRevB.101.041403

Introduction. Topological phenomena, such as the quantum Hall effect [1] and Thouless' adiabatic pump [2], are characterized by the precise quantization of certain transport properties. Recently, periodic driving has emerged as a versatile tool to control the topological characteristics of quantum systems [3–20]. Such ‘‘Floquet’’ systems can be realized in a wide variety of physical settings, including cold atomic, optical, and electronic systems [21–24]. The extent to which Floquet systems may host quantized transport is an important direction of investigation.

Interestingly, periodically driven quantum systems host unique topological phases which cannot be realized by their static counterparts [5,8,25–38]. The richer topological classification of these systems is due to their discrete (rather than continuous) time translation symmetry, which is manifested as a periodicity of the quasienergy—the energylike variable that characterizes the Floquet spectrum. Crucially, this structure provides the basis for wholly new types of quantized transport phenomena, also without analogs in static systems.

The first example of a quantized transport phenomenon unique to periodically driven systems was uncovered in Ref. [2]. There, Thouless showed that the charge transmitted through an insulating one-dimensional system is quantized as an integer multiple of the fundamental charge when the system is adiabatically driven through a cycle in parameter space.

More recently, in Ref. [29] it was shown that two-dimensional, disordered, periodically driven systems host a unique topological phase called the anomalous Floquet Anderson insulator (AFAI). In the AFAI phase, all bulk Floquet eigenstates are localized, while chiral edge states run along the system's boundaries. The AFAI's chiral edge states exist at *all* quasienergies; each such chiral edge mode carries a quantized current when completely filled. In this work we show that, in a two-terminal transport setup, the AFAI carries a *net* quantized current $I = \mathcal{W}_{2D}/T$ in the limit of large source-drain bias

(see Fig. 1). Here \mathcal{W}_{2D} is the winding number invariant that characterizes two-dimensional (2D) periodically driven systems [25,29,39]. Associated with the quantized current, we find an inhomogeneous density profile in which the AFAI's right-moving chiral edge state is fully occupied, while the left-moving chiral edge state is empty. Importantly, while quantized pumping in the Thouless pump is found in the adiabatic limit, the large-bias quantized current carried by a driven system in the AFAI phase occurs for intermediate driving frequencies (comparable to the system's natural bandwidth).

The AFAI phase occurs in two-dimensional systems, whose dynamics are governed by a time-periodic Hamiltonian $H_S(t) = H_S(t + T)$, where T is the driving period. The periodic driving gives rise to a unitary evolution $U_S(t) = \mathcal{T}e^{-i\int_0^t dt' H_S(t')}$, where \mathcal{T} denotes time ordering. The spectrum of the Floquet operator $U_S(T)$, given by $U_S(T)|\psi_n(0)\rangle =$

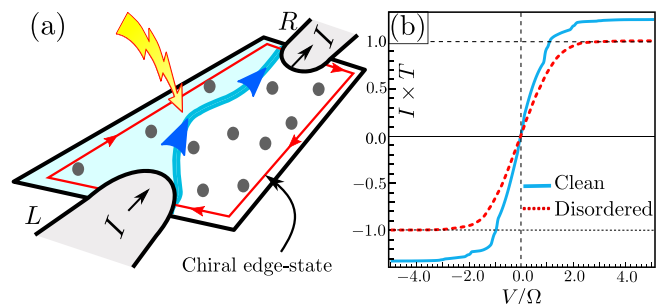


FIG. 1. Quantized transport in the AFAI phase. (a) Two-terminal transport setup. A large source-drain bias ensures that the edge states running from source to drain are fully filled, while those running from drain to source are empty. (b) Bias (V) dependence of the steady-state current, I , for clean (light blue) and fully localized (dark red) systems. In the disordered system the current saturates to the quantized value $I = 1/T$ for $V \gtrsim 2\Omega$, where $\Omega = 2\pi/T$ is the driving frequency.

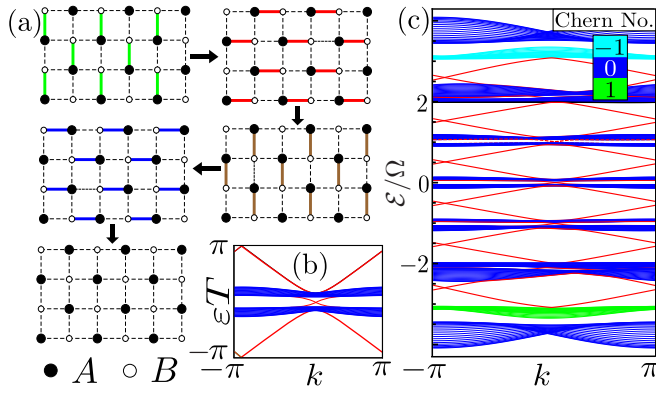


FIG. 2. Model of the AFAI phase. (a) Driving proceeds in five steps of equal length, $T/5$. In each step, the highlighted bonds are active with strength $J_{ij} = 5\pi/(2T)$, Eq. (2), while all others are set to 0. The sublattices A and B are denoted by black and white circles, respectively. (b) Quasienergy spectrum of H_S^{clean} , with $D = \pi/(2T)$. (c) Spectrum of the truncated extended zone (EZ) picture system Hamiltonian, H_S^{EZ} (with $M = 3$), see Eq. (9), in the absence of disorder. While the bands near $\mathcal{E} = 0$ have Chern number zero, close to the truncation we find bands with Chern numbers ± 1 .

$e^{-i\epsilon_n T} |\psi_n(0)\rangle$, defines the Floquet states $\{|\psi_n(t)\rangle\}$ and their quasienergies $\{\epsilon_n\}$.

To study quantized transport in the AFAI phase, we consider a finite region of AFAI connected to two wide-bandwidth (nondriven) leads, as shown in Fig. 1(a). The leads are indexed by $\lambda = \{L, R\}$, standing for the left and right leads, respectively. Dynamics of the combined system-lead setup are described by the Hamiltonian

$$H(t) = H_S(t) + \sum_{\lambda=L,R} H_\lambda + \sum_{\lambda=L,R} H_{S\lambda}, \quad (1)$$

where $H_S(t) = H_S(t + T)$ is the time-periodic Hamiltonian of the AFAI system, H_λ is the Hamiltonian describing lead λ , and $H_{S\lambda}$ describes the coupling between the system and lead λ . We treat each lead as an ideal Fermi reservoir, with filling characterized by an equilibrium Fermi-Dirac distribution with chemical potential μ_λ in lead λ . Specific forms for the Hamiltonian terms above will be given below. Throughout this paper, we use $e, \hbar = 1$.

The AFAI phase can be realized by a variety of driving protocols and experimental platforms, including solid-state and cold atoms. For concreteness and simplicity, here we use the square lattice tight-binding model introduced in Ref. [29]. In this model, the AFAI is described by the Hamiltonian $H_S(t) = H_S^{\text{clean}}(t) + \sum_i w_i c_i^\dagger c_i$, where c_i^\dagger (c_i) is the fermionic creation (annihilation) operator for site i , and w_i is a normally distributed on-site disorder potential with zero mean and standard deviation w . The clean (disorder-free) Hamiltonian is given by

$$H_S^{\text{clean}}(t) = \sum_{\langle ij \rangle} J_{ij}(t) c_i^\dagger c_j + \sum_i D n_i c_i^\dagger c_i, \quad (2)$$

where $\{J_{ij}(t)\}$ are time-dependent nearest-neighbor hopping amplitudes. It is convenient to define two sublattices A and B on the square lattice (see Fig. 2). The piecewise-constant

amplitudes $J_{ij}(t)$ connecting the two sublattices are modulated according to the five-step cycle depicted in Fig. 2(a), where each step has length $T/5$. Within each step, all nonzero hopping amplitudes (bold bonds) have strength $J = \frac{5\pi}{2T}$; in the fifth interval, all $J_{ij} = 0$. The parameter D is a staggered potential on the A and B sublattices, with $n_i = +1$ (-1) for the A (B) sublattice. We emphasize that the quantization of the current at large bias is universal and independent of the specific model; a cold atom realization based on Refs. [40,41] is analyzed in the Supplemental Material [42].

Within the AFAI phase, realized for nonzero w below a critical value [29], the system in an open geometry exhibits chiral edge states in coexistence with a fully localized bulk. These chiral edge states are illustrated in the example spectra for the clean system ($w = 0$) in an infinite-strip geometry, shown in Fig. 2(b).

We now study the steady-state current transported through the system when it is coupled to leads. To this end, we consider the Heisenberg equations of motion for the operators $c_j(t) = U(t)c_j(t_0)U^\dagger(t)$ and $a_j^\lambda(t) = U(t)a_j(t_0)U^\dagger(t)$, where a_j^λ is the fermionic annihilation operator on site j of lead λ , and $U(t) = \mathcal{T}e^{-i\int_0^t dt' H(t')}$ is the evolution operator for the full Hamiltonian, Eq. (1).

To simplify notation we introduce the operator vectors $\mathbf{a}_\lambda = (\dots a_{\lambda i} \dots)^T$ and $\mathbf{c} = (\dots c_i \dots)^T$, and express the system, lead, and system-lead coupling Hamiltonians in Eq. (1) as $H_S(t) = \mathbf{c}^\dagger \mathbf{H}_S(t) \mathbf{c}$, $H_\lambda = \mathbf{a}_\lambda^\dagger \mathbf{H}_\lambda \mathbf{a}_\lambda$, and $H_{S\lambda} = \mathbf{c}^\dagger \mathbf{H}_{S\lambda} \mathbf{a}_\lambda + \text{H.c.}$, respectively. We leave the specific forms of the matrices \mathbf{H}_λ and $\mathbf{H}_{S\lambda}$ unspecified for now.

The macroscopic leads are assumed to be attached in the very long past, such that the system operators $\mathbf{c}(t)$ are completely determined by the distribution in the leads; i.e., there is no memory of any initial occupations in the system. We then write a formal solution for the Heisenberg equation of motion, $i\dot{\mathbf{c}} = \mathbf{H}_S \mathbf{c} + \sum_\lambda \mathbf{H}_{S\lambda} \mathbf{a}_\lambda$:

$$\mathbf{c}(t) = \int dt' \mathbf{G}(t, t') \left[\sum_\lambda \mathbf{H}_{S\lambda} \mathbf{g}_\lambda(t' - t_0) \mathbf{a}_\lambda(t_0) \right], \quad (3)$$

where $\mathbf{g}_\lambda(t) = -i \exp(-i\mathbf{H}_\lambda t) \theta(t)$ is the retarded propagator for lead λ and $\mathbf{G}(t, t')$ is the full retarded Green's function within the system.

For the calculations below, it is convenient to furthermore define the Fourier-transformed Floquet Green's function,

$$\mathbf{G}^{(k)}(\mathcal{E}) = \frac{1}{T} \int_0^T dt \int_{-\infty}^{\infty} ds \mathbf{G}(t, t-s) e^{i\mathcal{E}s} e^{ik\Omega t}, \quad (4)$$

and

$$\xi_\lambda(\mathcal{E}) = \mathbf{H}_{S\lambda} \rho_\lambda(\mathcal{E}) \mathbf{H}_{S\lambda}^\dagger, \quad (5)$$

where $\rho_\lambda(\mathcal{E}) = \sum_n \delta(\mathcal{E} - E_{\lambda n}) |\lambda n\rangle \langle \lambda n|$ captures the density of states of lead λ , with $\mathbf{H}_\lambda |\lambda n\rangle = E_{\lambda n} |\lambda n\rangle$ [43].

The net current flowing into the right lead, averaged over one period, is given by

$$I = \frac{1}{T} \int_0^T dt i \langle [H(t), N_R(t)] \rangle, \quad (6)$$

where $N_R(t) = \mathbf{a}_R^\dagger(t) \mathbf{a}_R(t)$ is the number operator for the right lead. Through Eq. (3) we express the *system* operators $\mathbf{c}(t)$

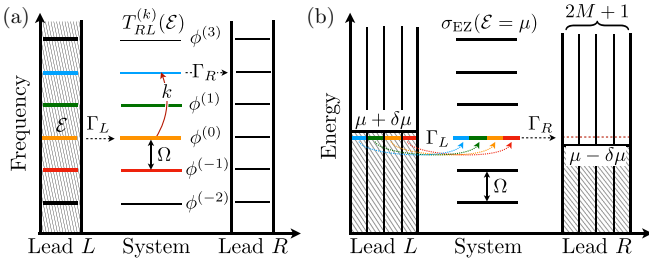


FIG. 3. Considerations leading to the sum rule in Eq. (10). (a) Transport through the driven system. A particle with energy \mathcal{E} enters the system from the left lead via the component $|\phi_\varepsilon^{(0)}\rangle$ of a Floquet state $|\psi_\varepsilon(t)\rangle$, with quasienergy $\varepsilon \approx \mathcal{E}$. The particle then scatters into a state with energy $\mathcal{E} + k\Omega$ in the right lead via its coupling to the component $|\phi_\varepsilon^{(k)}\rangle$. (b) Transport in the static extended zone (EZ) system [see Eq. (9)]. The EZ lead consists of $2M + 1$ identical channels, shifted in energy by integer multiples of Ω . A state in the lead with energy μ and harmonic index n is coupled to the component $|\Phi_\mu^{(n)}\rangle$ of the eigenstate $|\psi_\mu^{\text{EZ}}\rangle$ of $\mathcal{H}_S^{\text{EZ}}$ with eigenvalue μ .

as linear combinations of the *lead* operators $\mathbf{a}_\lambda(t_0)$ in the distant past (we take $t_0 \rightarrow -\infty$). Similarly, the lead operators $\mathbf{a}_\lambda(t)$ can be written in terms of $\mathbf{a}_\lambda(t_0)$. We assume that the state in each lead λ is given by a Fermi distribution f_λ with chemical potential μ_λ and temperature T_λ : $\langle a_{\lambda n}^\dagger(t_0) a_{\lambda m}(t_0) \rangle = \delta_{nm} f_\lambda(\varepsilon_{\lambda n})$, where $a_{\lambda n}^\dagger$ creates an electron in eigenstate $|\lambda n\rangle$ in lead λ (see above). Using Eqs. (3)–(5) and the Fermi distributions for the leads, a standard calculation gives [44]

$$I = 2\pi \int_{-\infty}^{\infty} d\mathcal{E} \sum_k \{T_{\text{RL}}^{(k)}(\mathcal{E}) f_L(\mathcal{E}) - T_{\text{LR}}^{(k)}(\mathcal{E}) f_R(\mathcal{E})\},$$

$$T_{\lambda\lambda'}^{(k)}(\mathcal{E}) = \text{Tr}[\mathbf{G}^{(k)\dagger}(\mathcal{E}) \xi_\lambda(\mathcal{E} + k\Omega) \mathbf{G}^{(k)}(\mathcal{E}) \xi_{\lambda'}(\mathcal{E})]. \quad (7)$$

Here $T_{\lambda\lambda'}^{(k)}(\mathcal{E})$ is the probability for an electron at energy \mathcal{E} to be transmitted from lead λ' to lead λ , along with the absorption of k photons from the driving field.

As we now show, the steady-state time-averaged current carried by the AFAI, Eq. (7), is *quantized* in the limit of large bias, $V \rightarrow \infty$, with $\mu_L = V/2$, $\mu_R \rightarrow -V/2$. In this limit we may set $f_L(\mathcal{E}) = 1$ and $f_R(\mathcal{E}) = 0$, yielding

$$I = \int_{-\infty}^{\infty} d\mathcal{E} \sigma(\mathcal{E}), \quad \sigma(\mathcal{E}) = 2\pi \sum_k T_{\text{RL}}^{(k)}(\mathcal{E}). \quad (8)$$

In the following, we show the quantization of the current by relating $\sigma(\mathcal{E})$ to the differential conductance of an associated *static* system. For illustration, we first consider the dominant processes contributing to $\sigma(\mathcal{E})$ [see Fig. 3(a)]. In each process a particle in the left lead with energy \mathcal{E} scatters into a Floquet state of the system with quasienergy $\varepsilon \approx \mathcal{E} + n\Omega$ [45]. The integer n is determined by our convention for Floquet states, $|\psi_\varepsilon(t)\rangle = e^{-i\mathcal{E}t} \sum_m |\phi_\varepsilon^{(m)}\rangle e^{-i\Omega mt}$, with $-\Omega/2 \leq \varepsilon < \Omega/2$. The scattering process thus proceeds through the coupling between the lead state and the component $|\phi_\varepsilon^{(-n)}\rangle$. The particle then scatters into a state in the right lead with energy $\mathcal{E} + k\Omega$, via its coupling to the component $|\phi_\varepsilon^{(k-n)}\rangle$. Thus, in the process of scattering from the left to the right lead the particle absorbs k photons from the time-periodic drive. The collection of processes involving such changes in

the particle's energy is captured by the sum appearing in the definition of $\sigma(\mathcal{E})$, Eqs. (7) and (8).

We now reexpress the current, Eq. (8), as $I = \int_{-\Omega/2}^{\Omega/2} (dI/d\varepsilon) d\varepsilon$, with $dI/d\varepsilon = \sum_n \sigma(\mathcal{E} + n\Omega)$. The quantity $dI/d\varepsilon$ can be related to the differential conductance of a *static* system, which describes the periodically driven system in an “extended zone” (EZ) frequency-space picture. The Hamiltonian of the static EZ system is given by $\mathcal{H}^{\text{EZ}} = \sum_{m,n}^M H_{mn}^{\text{EZ}} |m\rangle\langle n|$, where the sum runs over $-M \leq n, m \leq M$, and

$$H_{mn}^{\text{EZ}} = -\delta_{mn} n\Omega + \int_0^T dt \frac{d}{dt} e^{i(m-n)\Omega t} H(t). \quad (9)$$

The operator \mathcal{H}^{EZ} acts in enlarged Hilbert space, which is a tensor product of the original Hilbert space and a $(2M + 1)$ -dimensional auxiliary space, which we call the harmonic space.

As in Eq. (1), we write $\mathcal{H}^{\text{EZ}} = \mathcal{H}_S^{\text{EZ}} + \sum_\lambda \mathcal{H}_{S\lambda}^{\text{EZ}} + \sum_\lambda \mathcal{H}_\lambda^{\text{EZ}}$. An eigenstate of $\mathcal{H}_S^{\text{EZ}}$ with energy \mathcal{E} can be expanded as $|\psi_\varepsilon^{\text{EZ}}\rangle = \sum_n |\Phi_\varepsilon^{(n)}\rangle \otimes |n\rangle$. The eigenvalues of $\mathcal{H}_S^{\text{EZ}}$ in the range $-\Omega/2 \leq \mathcal{E} < \Omega/2$ approximate the *quasienergy* spectrum of $U_S(T) = \mathcal{T} e^{-i \int_0^T dt H_S(t)}$, becoming exact for $M \rightarrow \infty$. Importantly, in this limit, for each $|\psi_\varepsilon^{\text{EZ}}\rangle$ there is a corresponding partner Floquet state with quasienergy $\varepsilon = \mathcal{E} + m\Omega$ (with $|\varepsilon| \leq \Omega/2$) in the original driven problem: $|\psi_\varepsilon(t)\rangle = e^{-i\mathcal{E}t} \sum_n |\phi_\varepsilon^{(n)}\rangle e^{-i\Omega nt}$, with $|\phi_\varepsilon^{(n-m)}\rangle = |\Phi_\varepsilon^{(n)}\rangle$.

We now relate the relevant transport processes in the static EZ and Floquet pictures (see Fig. 3). Consider the differential conductance, $\sigma_{\text{EZ}}(\mu)$, of the EZ system described by \mathcal{H}^{EZ} . Since the lead is not driven, the spectrum of $\mathcal{H}_\lambda^{\text{EZ}}$ consists of $2M + 1$ copies of that of H_λ , shifted by integer multiples of Ω ; it can thus be viewed as a lead with many channels, labeled by the harmonic index. We define $\sigma_{\text{EZ}}(\mu)$ by taking the Fermi level of the left and the right EZ leads to be $\mu + \delta\mu$ and $\mu - \delta\mu$, and take $-\Omega/2 \leq \mu < \Omega/2$ throughout [46].

Consider now the dominant processes contributing to $\sigma_{\text{EZ}}(\mu)$. The system-lead coupling $\mathcal{H}_{S\lambda}^{\text{EZ}}$ conserves the harmonic index. Therefore, a lead state with energy \mathcal{E} and harmonic index n (which corresponds to a state of the physical lead with energy $\mathcal{E} - n\Omega$) is coupled to the state $|\psi_\varepsilon^{\text{EZ}}\rangle$ through the component $|\Phi_\varepsilon^{(n)}\rangle$. To obtain $\sigma_{\text{EZ}}(\mu)$, we sum the contributions of states with energies close to μ from all harmonic-index channels in both leads. Using the correspondence between $\{|\psi_\mu^{\text{EZ}}\rangle\}$ and $\{|\psi_\mu(t)\rangle\}$, for $M \gg 1$, we thus obtain [42]

$$\sum_n \sigma(\mu + n\Omega) = \sigma_{\text{EZ}}(\mu). \quad (10)$$

Importantly, in the EZ picture, $\sigma_{\text{EZ}}(\mu)$ is just the two-terminal differential conductance of a disordered Chern insulator, with μ lying in a mobility gap. To see why this is the case, consider the spectrum of $\mathcal{H}_S^{\text{EZ}}$ in the AFAI phase. In the spectral range $-\Omega/2 \leq \mu < \Omega/2$ it exhibits two important properties: (i) all bulk states are localized [48], and (ii) chiral edge states exist at all energies within this range. These two properties of $\mathcal{H}_S^{\text{EZ}}$ are a direct consequence of the properties of $U_S(T)$ in the AFAI phase. Since in the EZ picture the number of edge states corresponds to the total Chern number of all bulk states below μ , the spectrum of

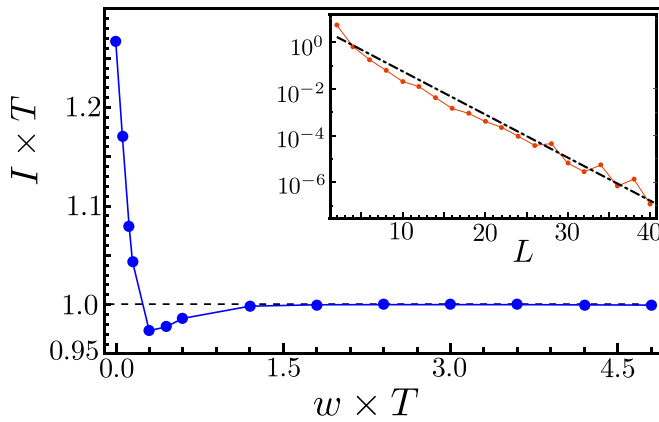


FIG. 4. Steady-state current vs disorder strength w , for $V \gg \Omega$. As w is increased from zero, the steady-state current (averaged over a period) rapidly approaches the quantized value of $1/T$ [47]. The sample has dimensions $L \times W = 40 \times 20$ sites. The leads are taken to have widths $W_0 = W/2$. Inset: Bulk contribution to the steady-state current, computed using a cylindrical geometry with contacts on opposite edges of the cylinder, for $w = 4.5/T$. Exponential decay of the bulk contribution with increasing L indicates that the system is in the localized regime.

$\mathcal{H}_S^{\text{EZ}}$ must contain a band with nontrivial Chern number at an energy near the harmonic space truncation at $n = -M$. The quantized two-terminal differential conductance of such a Chern insulator [49], $\sigma^{\text{EZ}}(\mu) = \mathcal{W}_{2\text{D}}$, together with Eq. (8), yields $I = \sum_n \int_{-\Omega/2}^{\Omega/2} d\mathcal{E} \sigma(\mathcal{E} + n\Omega) = \mathcal{W}_{2\text{D}}/T$.

For the model given in Fig. 2(a), the above considerations are exemplified by inspecting the spectrum of the corresponding $\mathcal{H}_S^{\text{EZ}}$ (without disorder), given in Fig. 2(c). Here we find a single chiral edge in the spectral range $-\Omega/2 \leq \mathcal{E} < \Omega/2$; in this spectral range, the Chern numbers of the bands are all zero. However, the highlighted bands near the bottom and top of the spectrum, which are strongly affected by the truncation, have Chern numbers ± 1 .

Numerical simulations. To support the arguments above, we now numerically study the steady-state current. We simulate the model described above, Eq. (1), for a range of system sizes and disorder strengths w (see Fig. 4). We take $D = \pi/(2T)$, and the leads to have constant density of states, $\rho_{0\lambda} = 1/J$. The lead-system coupling $\mathbf{H}_{S\lambda}$ is taken to yield $\xi_\lambda(\mathcal{E}) = \sum_{\mathbf{r} \in W_0} \rho_{0\lambda} |\mathbf{r}\rangle \langle \mathbf{r}|$, where the sum runs over W_0 system sites directly adjacent to lead λ [see Fig. 5(a)].

In the presence of disorder, all bulk states are localized and the current through the bulk vanishes exponentially with the distance between the leads. To probe this, we computed the current in a cylindrical geometry, with leads attached at opposite ends of the cylinder such that there were no edge states connecting the source and drain (shown in the inset of Fig. 4). As shown in Fig. 1(b) and the main panel of Fig. 4, for the Hall bar geometry of Fig. 1(a) the total current through the system saturates to the quantized value $I = 1/T$ in the insulating regime, for large (finite) bias.

As explained above, a quantized current is expected to flow in the AFAI when the edge states exiting from the left lead are completely filled, while those exiting the right lead are empty. We confirm this picture (for a typical disorder realization)

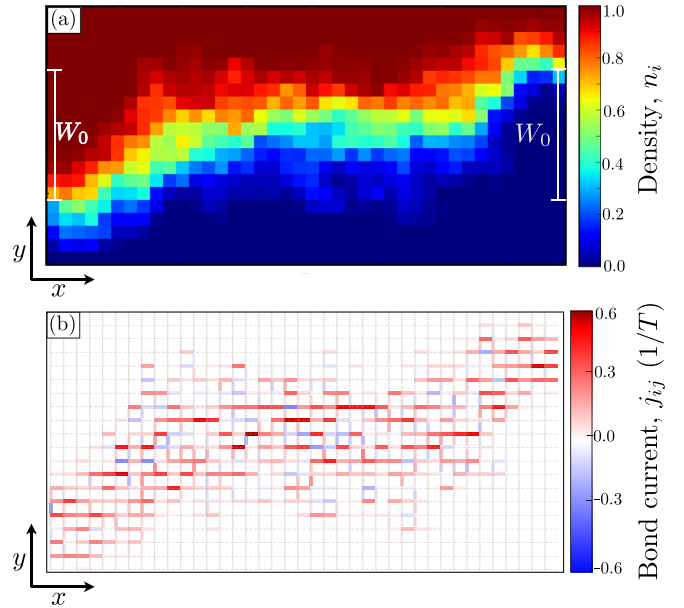


FIG. 5. (a) Map of the steady-state period-averaged density, n_i , for $w = 4.5/T$. The large bias between the leads, $V \gg \Omega$, ensures that the edge state running from source to drain is fully occupied, while that running from drain to source is empty. (b) The period-averaged bond currents j_{ij} (see text). The current density is concentrated at the interface between fully occupied and empty regions.

by mapping out the steady-state time-averaged local density, $n_i = \frac{1}{T} \int_0^T dt \langle c_i^\dagger(t) c_i(t) \rangle$, in Fig. 5(a). This situation is realized for “good” contacts, with appropriately strong couplings ξ_λ and large enough contact width W_0 (see Fig. 5 and the Supplemental Material [42]).

To further investigate the spatial distribution of the current, we map out the period-averaged bond current density, $j_{ij} = \frac{1}{T} \int_0^T dt 2\text{Im}[J_{ij}(t) \langle c_i^\dagger(t) c_j(t) \rangle]$ [see Eq. (2)]. As shown in Fig. 5(b), the current density is concentrated at the boundary of the filled and empty regions. This result may at first seem counterintuitive since (a) all states in the bulk are localized and (b) we expect the quantized current to be carried by the chiral edge states. However, it is crucial to remember that the local current density $j_{ij}(t)$ includes contributions of both transport currents and magnetization current [39,50]. The quantized *transport current* is indeed carried by the chiral edge states, as they are the only delocalized states in the system [42].

Summary. In this work we demonstrated theoretically a topological quantized transport phenomenon, occurring in disordered two-dimensional periodically driven systems. In contrast to the equilibrium quantized Hall *conductivity*, in the AFAI phase, which occurs in a system *far from equilibrium*, we find a quantized *current* in the limit of large bias [51]. Looking ahead, disorder-induced localization may provide a route for stabilizing interacting Floquet phases of matter by suppressing energy absorption from the periodic drive. Recently, several works proposed interacting analogs of the AFAI [52–56]. Determining whether quantized transport and other response functions can be used to probe these interacting phases will be crucial for further progress in the field.

Acknowledgments. A.K. acknowledges the support from the Indian Institute of Technology–Kanpur and was supported in part at the Technion by a fellowship of the Israel Council for Higher Education. N.H.L. acknowledges support from the People Programme (Marie Curie Actions) of the European Union’s Seventh Framework Programme (No. FP7/2007–2013) under REA Grant Agreement No. 631696, and from the Israeli Center of Research Excellence (I-CORE) “Circle of Light.” N.H.L. and E.B. acknowledge support from the

European Research Council (ERC) under the European Union Horizon 2020 Research and Innovation Programme (Grant Agreement No. 639172). M.R. gratefully acknowledges the support of the European Research Council (ERC) under the European Union Horizon 2020 Research and Innovation Programme (Grant Agreement No. 678862), and the Villum Foundation. M.R. and E.B. acknowledge support from CRC 183 of the Deutsche Forschungsgemeinschaft.

-
- [1] K. v. Klitzing, G. Dorda, and M. Pepper, *Phys. Rev. Lett.* **45**, 494 (1980).
- [2] D. J. Thouless, *Phys. Rev. B* **27**, 6083 (1983).
- [3] W. Yao, A. H. MacDonald, and Q. Niu, *Phys. Rev. Lett.* **99**, 047401 (2007).
- [4] T. Oka and H. Aoki, *Phys. Rev. B* **79**, 081406(R) (2009).
- [5] T. Kitagawa, E. Berg, M. Rudner, and E. Demler, *Phys. Rev. B* **82**, 235114 (2010).
- [6] J.-i. Inoue and A. Tanaka, *Phys. Rev. Lett.* **105**, 017401 (2010).
- [7] N. H. Lindner, G. Refael, and V. Galitski, *Nat. Phys.* **7**, 490 (2011).
- [8] L. Jiang, T. Kitagawa, J. Alicea, A. R. Akhmerov, D. Pekker, G. Refael, J. I. Cirac, E. Demler, M. D. Lukin, and P. Zoller, *Phys. Rev. Lett.* **106**, 220402 (2011).
- [9] Z. Gu, H. A. Fertig, D. P. Arovas, and A. Auerbach, *Phys. Rev. Lett.* **107**, 216601 (2011).
- [10] T. Kitagawa, T. Oka, A. Brataas, L. Fu, and E. Demler, *Phys. Rev. B* **84**, 235108 (2011).
- [11] N. H. Lindner, D. L. Bergman, G. Refael, and V. Galitski, *Phys. Rev. B* **87**, 235131 (2013).
- [12] P. Delplace, A. Gomez-Leon, and G. Platero, *Phys. Rev. B* **88**, 245422 (2013).
- [13] Y. T. Katan and D. Podolsky, *Phys. Rev. Lett.* **110**, 016802 (2013).
- [14] A. Kundu and B. Seradjeh, *Phys. Rev. Lett.* **111**, 136402 (2013).
- [15] M. Lababidi, I. I. Satija, and E. Zhao, *Phys. Rev. Lett.* **112**, 026805 (2014).
- [16] T. Iadecola, D. Campbell, C. Chamon, C.-Y. Hou, R. Jackiw, S.-Y. Pi, and S. V. Kusminskiy, *Phys. Rev. Lett.* **110**, 176603 (2013).
- [17] N. Goldman and J. Dalibard, *Phys. Rev. X* **4**, 031027 (2014).
- [18] A. G. Grushin, A. Gómez-León, and T. Neupert, *Phys. Rev. Lett.* **112**, 156801 (2014).
- [19] A. Kundu, H. A. Fertig, and B. Seradjeh, *Phys. Rev. Lett.* **113**, 236803 (2014).
- [20] P. Titum, N. H. Lindner, M. C. Rechtsman, and G. Refael, *Phys. Rev. Lett.* **114**, 056801 (2015).
- [21] Y. Wang, H. Steinberg, P. Jarillo-Herrero, and N. Gedik, *Science* **342**, 453 (2013).
- [22] M. C. Rechtsman, J. M. Zeuner, Y. Plotnik, Y. Lumer, D. Podolsky, F. Dreisow, S. Nolte, M. Segev, and A. Szameit, *Nature (London)* **496**, 196 (2013).
- [23] G. Jotzu, M. Messer, R. Desbuquois, M. Lebrat, T. Uehlinger, and D. Greif, *Nature (London)* **515**, 237 (2014).
- [24] R. Desbuquois, M. Messer, F. Görg, K. Sandholzer, G. Jotzu, and T. Esslinger, *Phys. Rev. A* **96**, 053602 (2017).
- [25] M. S. Rudner, N. H. Lindner, E. Berg, and M. Levin, *Phys. Rev. X* **3**, 031005 (2013).
- [26] J. K. Asboth, B. Tarasinski, and P. Delplace, *Phys. Rev. B* **90**, 125143 (2014).
- [27] D. Carpentier, P. Delplace, M. Fruchart, and K. Gawedzki, *Phys. Rev. Lett.* **114**, 106806 (2015).
- [28] F. Nathan and M. S. Rudner, *New J. Phys.* **17**, 125014 (2015).
- [29] P. Titum, E. Berg, M. S. Rudner, G. Refael, and N. H. Lindner, *Phys. Rev. X* **6**, 021013 (2016).
- [30] V. Khemani, A. Lazarides, R. Moessner, and S. L. Sondhi, *Phys. Rev. Lett.* **116**, 250401 (2016).
- [31] R. Roy and F. Harper, *Phys. Rev. B* **94**, 125105 (2016).
- [32] D. V. Else and C. Nayak, *Phys. Rev. B* **93**, 201103(R) (2016).
- [33] C. W. von Keyserlingk and S. L. Sondhi, *Phys. Rev. B* **93**, 245145 (2016).
- [34] A. C. Potter, T. Morimoto, and A. Vishwanath, *Phys. Rev. X* **6**, 041001 (2016).
- [35] R. Roy and F. Harper, *Phys. Rev. B* **96**, 155118 (2017).
- [36] C. W. von Keyserlingk, V. Khemani, and S. L. Sondhi, *Phys. Rev. B* **94**, 085112 (2016).
- [37] D. V. Else, B. Bauer, and C. Nayak, *Phys. Rev. Lett.* **117**, 090402 (2016).
- [38] J. Zhang, P. W. Hess, A. Kyprianidis, P. Becker, A. Lee, J. Smith, G. Pagano, I.-D. Potirniche, A. C. Potter, and A. Vishwanath, *Nature (London)* **543**, 217 (2017).
- [39] F. Nathan, M. S. Rudner, N. H. Lindner, E. Berg, and G. Refael, *Phys. Rev. Lett.* **119**, 186801 (2017).
- [40] A. Quelle, C. Weitenberg, K. Sengstock, and C. Morias Smith, *New J. Phys.* **19**, 113010 (2017).
- [41] S. Krinner, D. Stadler, D. Husmann, J. Brantut, and T. Esslinger, *Nature (London)* **517**, 64 (2015).
- [42] See Supplemental Material at <http://link.aps.org/supplemental/10.1103/PhysRevB.101.041403> for a detailed derivation of the sum rule; discussion of an alternative model suitable for cold-atomic realization; dependence on the contact width and the aspect ratio; and a discussion on magnetization current.
- [43] In the $\{ \lambda n \}$ basis, we have $[\rho_\lambda(\mathcal{E})]_{nm} = \frac{-1}{2\pi i} \text{Im} \{ [g_\lambda(\mathcal{E})]_{nm} \}$.
- [44] S. Kohler, J. Lehmann, and P. Hanggi, *Phys. Rep.* **406**, 379 (2005).
- [45] Due to finite coupling strength, the energy conservation condition is broadened on the scale of the tunneling rate.
- [46] The states of \mathcal{H}_L^{EZ} are populated according to a Fermi-Dirac distribution with chemical potential $\mu + \delta\mu$ regardless of their harmonic index (and similarly for the right lead).
- [47] The negative overshoot at low disorder is due to the aspect ratio of the system (see Supplemental Material). Note that at very strong disorder, the system undergoes a transition to a

- trivial insulator, where the current vanishes. This transition was studied in Ref. [29].
- [48] Note that delocalized states exist at energies close to the truncation. However, for sufficiently large M their energies do not lie in the window $\Omega/2 < \mu < \Omega/2$, and therefore do not contribute to transport.
- [49] The quantized value is obtained for sufficiently large contact length.
- [50] D. Xiao, M.-C. Chang, and Q. Niu, *Rev. Mod. Phys.* **82**, 1959 (2010).
- [51] The I - V characteristic of quantum Hall systems is generically nonlinear at large source-drain biases, but the current does not saturate to a universal quantized value as it does for the AFAI.
- [52] H. C. Po, L. Fidkowski, T. Morimoto, A. C. Potter, and A. Vishwanath, *Phys. Rev. X* **6**, 041070 (2016)
- [53] H. Chun Po, L. Fidkowski, A. Vishwanath, and A. C. Potter, *Phys. Rev. B* **96**, 245116 (2017).
- [54] L. Fidkowski, H. Chun Po, A. C. Potter, and A. Vishwanath, *Phys. Rev. B* **99**, 085115 (2019).
- [55] A. C. Potter, A. Vishwanath, and L. Fidkowski, *Phys. Rev. B* **97**, 245106 (2018).
- [56] F. Harper and R. Roy, *Phys. Rev. Lett.* **118**, 115301 (2017).